



Artur Palha
Technological Physicist,
LNEC, Lisbon, Portugal



Conceição J. E. M.
Fortes
Civil Engineer, LNEC,
Lisbon, Portugal



Paulo R. F. Teixeira
Professor, Post
graduated Program in
Ocean Engineering,
FURG, Brazil



Liliana V. Pinheiro
Civil Engineer, LNEC,
Lisbon, Portugal

Irregular wave propagation at Torres-Mostardas beach, Brazil

A. Palha, C. J. E. M. Fortes, P. R. F. Teixeira and L. V. Pinheiro

The parabolic mild-slope model Refdif_S simulates the propagation and deformation of irregular waves in coastal regions with variable water depth. PY_Refdif_S software tool is an extension of the model, using a multi-grid approach in order to achieve a more efficient and applicable model to large areas and a large set of different wave conditions. The tool is made up of several Python routines that automatically build multiple grids, prepare data files and execute Refdif_S for several sea states. The model was applied to the study of irregular wave propagation from offshore to nearshore in the region of Torres-Mostardas, Brazil. For a range of irregular incident sea states, several calculations with the tool were performed. The wave field and local sea states were characterised in that area. Based on this application, advantages and limitations of the tool are analysed.

1. INTRODUCTION

The knowledge of the wave climate is of major importance on coastal and harbour engineering problems. Numerical models are important tools to simulate different scenarios and to predict the effects of human and natural actions. In fact, the study of morphodynamic processes and coastline evolution, the design of breakwaters, harbours, marinas or wave power energy systems, and coastal and harbour management, are some of the situations where knowledge of the wave propagation field is essential.

Numerical models for the propagation and deformation of waves are often used with regular (or monochromatic) waves only, whether because the model is unable to propagate irregular waves or for simplification purposes. A real sea state is, however, quite different from a monochromatic wave field, which is only represented by a single wave direction, wave height and wave period. A real sea state is characterised by an irregular shape, composed of a great variety of waves, moving in several different directions, and composed of a group of frequencies, phases and amplitudes. Goda (1985), Vincent and Briggs (1989) and Panchang *et al.* (1990) showed, in analytical and experimental ways, that the substitution of a sea state by a monochromatic wave can induce important errors in the characterisation of wave action. Thus, the consideration of irregular wave characteristics would lead to an improvement of the numerical results.

There are several models capable of simulating the propagation

and deformation of an irregular sea state, such as phase-averaged models (Swan: Booij *et al.*, 1999) or phase resolving models (Ilic and Chadwick, 1995; Kirby and Ozkan, 1994; Kirby *et al.*, 1998; Lee and Williams, 2002; Li *et al.*, 1993; Lynett and Liu, 2004; Walkley, 1999). In general, the first ones are used to simulate the spectral wave propagation over large areas but since they are based upon the wave action balance equation, they propagate an average quantity of energy without considering the shape of the wave. The second ones can propagate the wave characteristics themselves, but they have higher computational cost. Phase resolving models based upon the parabolic approximation of the mild-slope equation are less demanding than elliptic mild-slope models or Boussinesq-type models.

The parabolic model Refdif_S (Kirby and Ozkan, 1994) was used in this study, as it is a model that is able to simulate the propagation of irregular sea states in areas of large dimensions in a reasonable amount of time and its code is freely available. Furthermore, this model simulates the shoaling of irregular waves in regions of variable depth, taking into account the effects of refraction, diffraction and wave breaking. The method used is the one of linear superposition, developed by Goda (1985). This method is based on the hypothesis that each spectral component behaves linearly and independently of all the others. According to this method, the irregular sea state is characterised by an incident directional and frequency spectrum, which is decomposed in discrete spectral components, each carrying the same amount of energy. These discrete components are then propagated individually by a regular wave model and afterwards assembled together, in order to get the irregular wave field. In the case of Refdif_S, the regular wave model used is Refdif (Dalrymple and Kirby, 1991).

However, the Refdif_S model has some limitations: (a) the propagation of irregular waves is associated with several spectral components which consume significant central processor unit (CPU) time and memory storage; (b) the model cannot be applied to domains discretised by more than one finite-difference grid (which does not happen with the REFDIF regular model). These limitations restrict the application of the irregular wave model to large coastal areas, but unlike other more sophisticated models, these limitations can be overcome by using multigrid techniques and some automatic manipulation of data.

In order to solve these difficulties, the PY_Refdif_S software tool was developed, which is an extension of the Refdif_S model. PY_Refdif_S is composed of several routines developed in the Python programming language and performs the automatic preparation of data files of the model, its execution on a Unix workstation instead of a personal computer and transfer of results and data between the Windows and the Unix environment. Moreover, the application of the model in large areas is also achieved by using a multi-grid technique to discretise the whole area of interest. To summarise, PY_Refdif_S is a software tool to enlarge the range of applications of the Refdif_S model, but this kind of methodology can also be applied with other models with minor adjustments.

The present paper provides a general description of the PY_Refdif_S tool and its application to study the irregular wave propagation in the region of Torres-Mostardas in Rio Grande do Sul, Brazil. The area of Rio Grande do Sul is characterised by a monotonous and gentle undulating barrier coast, oriented north-east-south-west and subject to dominant swell waves generated in southern latitudes, and wind-generated waves produced by strong spring-summer sea breezes from the north-east. The coast is microtidal with semi-diurnal tides that have a mean range of only 0.5 m. Consequently, sediment transport and deposition along the open coast is primarily dominated by wave action. Notice that this region, from Torres to Mostardas, is a very large area with 250 km long shoreline. Well-sorted fine quartz sands dominate in the Rio Grande do Sul beaches. Morphodynamically, the beaches vary from intermediate to dissipative stages.

As for this region, the information about the wave regime is almost non-existent; the incident wave characteristics were based upon the work of Fontoura (2004). In that work, the frequency distributions of sea states (wave height, period and direction), for the period between 26 September and 25 December 2001, are presented. Calculations were performed from offshore to nearshore in the region of Torres-Mostardas for peak periods in the range 5–12 s and mean wave directions between south and north-east, using the most frequent significant wave height which is of 1.75 m and considering the yearly mean tide level. The results consist of the significant wave heights and mean wave directions in the study region. These calculations permit a characterisation of the wave field from offshore to inshore for several incident irregular waves and the definition of the local sea states in front of the Torres-Mostardas beach, by wave transformation of the offshore sea states of Fontoura (2004).

2. THE PY_REFDIF_S SOFTWARE TOOL

The PY_Refdif_S software tool is based on the Refdif_S irregular wave propagation model (Kirby and Ozkan, 1994). PY_Refdif_S permits the application of the Refdif_S model to large areas (discretised with multiple finite-difference grids) and reduces the computing time of each calculation by using a Unix workstation instead of a personal computer.

For that purpose, PY_Refdif_S has several sub-routines written in the Python programming language which allow the following actions.

- (a) Automatic procedures for the preparation of data files, the

execution of the model, and the transfer of results and data between Windows and Unix-like environments.

- (b) The application of PY_Refdif_S to regions where the computational domain is discretised with multiple grids. This is very important, especially for large study areas and with regard to offshore waves propagating inshore.

Figure 1 presents a simplified scheme of PY_Refdif_S running on a Corvus dedicated server (a Unix workstation).

In this section, the PY_Refdif_S software tool is described, starting with the description of the Refdif_S model, its advantages and limitations, followed by the extensions added to the model that make the PY_Refdif_S software tool.

2.1. The Refdif_S model

The Refdif_S model (Kirby and Ozkan, 1994) is a numerical model based on the linear superposition method (Goda, 1985), which simulates the propagation and transformation of random waves over regions of variable depth. It is particularly applicable to regions in which the incoming random sea propagates over a complicated bathymetry towards the shore.

Using an offshore incident directional spectrum, the model simulates the evolution of irregular waves over a gently sloping bottom by using the equi-energetic method (Kirby and Ozkan, 1994). The methodology includes the following steps.

- (a) Definition and division of the offshore incident directional spectrum into several regular wave components, using the equi-energetic method (Grassa, 1992).
- (b) Use of the regular wave model Refdif (Dalrymple and Kirby, 1991), to predict the evolution of each wave component independently.
- (c) Combination of the results of Refdif for all the wave components.

The Refdif_S structure is based on a module for calculation of the directional and frequency spectrum, the Specgen module, and a module for the propagation of each component of the spectra and combination of those results, the Refdif_S module. A more detailed description is now presented.

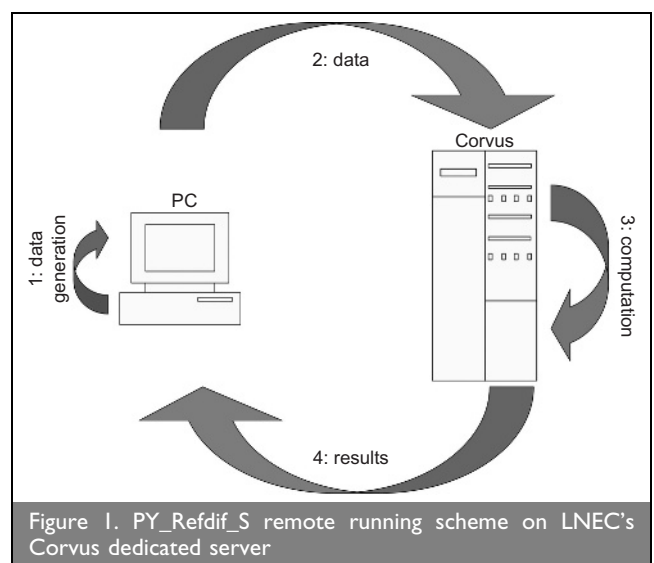


Figure 1. PY_Refdif_S remote running scheme on LNEC's Corvus dedicated server

- (a) Specgen: this module is responsible for the definition of the incident directional and frequency spectrum, and its subdivision in equal energy bins, through the equi-energetic procedure (Grassa, 1992).
- (i) The chosen functions for the description of the directional spectrum are the Texel, Marsen and Arsloe (TMA) spectrum in frequency (Bouws *et al.*, 1985), $S(f)$, and the Borgman's directional spreading function (Kirby and Ozkan, 1994), $D(\theta)$.
- (ii) After its definition, the incident directional spectrum will be divided into equal energy bins (which correspond to spectral components) (Grassa, 1992). The frequency and direction spectra are divided in several frequency (N_f) and directional (N_θ) intervals, associated with a certain wave height and wave period. The number of total spectral components is $N = N_f \times N_\theta$. Care needs to be taken to ensure there is the necessary number of components to obtain a good estimation of the referred spectra. In Zóximo (2003), it was noticed that the number of frequency and directional components has great influence on the model results.
- (b) Refdif_S: the propagation of each spectral component is made with the Refdif regular wave model (Dalrymple and Kirby, 1991), and combines the results of all the components. The principal characteristics of the regular wave model Refdif are listed here.
- (i) It is based on the parabolic approximation of the mild-slope equation of Berkhoff (1972), extended by Kirby (1986). This model takes into account refraction, diffraction, wave currents and wave breaking, for example. The equations are solved by a finite-difference mode, using a regular grid for the discretisation and an implicit iterative line-line scheme in the wave propagation direction.
- (ii) The wave breaking and the bottom friction are incorporated in the model by an extra term. For wave breaking, the model follows the formulation of Thornton and Guza (1983), whereas for turbulent bottom friction the formulation of Dean and Dalrymple (1984) is employed.
- (iii) The boundary conditions are a total reflection condition or an open boundary condition. The open boundary condition is used when there are no obstacles on that boundary; that is, if the computational domain on that boundary was extended it would contain only water with the same depth. Total reflection should be used when an obstacle exists in the boundary, for instance in regions where there is a wave breaker. In the case of the simulations presented here, only open boundary conditions were used.
- (iv) As for the initial conditions, one can specify a field of monochromatic waves or a field defined by a directional spectrum.

In conclusion, the Refdif_S model simulates the irregular wave propagation on mild-slope bottoms in the presence of currents, taking into account the refraction, diffraction (only in the perpendicular direction of the main direction of propagation) and shoaling wave dissipation (bottom friction and wave breaking).

The Refdif_S data include: (a) spectrum characteristics (peak

period, average direction, maximum frequency, significant wave height at the entrance of the domain, tide, the peak enhancement factor for the TMA spectrum, γ , the directional spreading parameter of the Borgman's spectrum, σ_m) and the number of components in frequency and direction (N_f and N_θ); (b) the grid characteristics; and (c) the bathymetry.

The model calculates the significant wave height, HS , complex amplitude, A , and the surface elevation, η , in each point of the domain.

For the model's application, one should ensure that

- (a) the bottom should have a mild slope (slope under 1:3)
- (b) the orientation of the grid should guarantee that the wave direction inside the grid does not exceed $\pm 60^\circ$ of the principal wave direction, due to the use of the large-angle parabolic approximation
- (c) the number of components in which the directional spectrum is divided should correctly define the spectrum.

2.1.1. Model limitations. Regarding the theoretical formulation, the main limitations of Refdif_S model are listed here.

- (a) The model does not take into account the wave reflection phenomenon because it cannot deal with the back-scattering of waves. Moreover, diffraction is only taken into account considering the normal wave direction; therefore it cannot be used in sheltered areas. Notice that the model is based upon the large-angle parabolic approximation of the mild-slope equation of Berkhoff (1972).
- (b) The model can only be applied to mild-slope bottoms, namely slopes of 1:3 or less.
- (c) The model is based on the linear superposition method (Goda, 1985), and so there is no generation of harmonics or non-linear interaction between the different spectral components.

Considering the execution of the model, the model limitations are identified.

- (a) The Refdif_S model can only be applied to domains which are discretised by a single finite-difference grid. This fact limits the application of the model in large areas.
- (b) The execution of the Refdif_S model on a personal computer is time-consuming, when it is applied to real test cases, which are usually large. Notice that for each single irregular wave condition the computation time is related to the number of the spectral components into which the spectrum is divided, and consequently to the CPU time associated with the propagation of each spectral component. As the computation time increases, the performance of the Refdif_S model decreases. This problem limits the application of the model to different irregular wave conditions.

2.2. PY_Refdif_S routines

2.2.1. The programming language choice. Scripting languages have become a powerful tool for the construction of flexible scientific software because they provide an interpreted programming environment. They can be easily interfaced with existing software written in C, C++ and Fortran, and can serve as a framework for modular software construction.

One of the more promising technologies to emerge in recent years is the use of common scripting languages such as Python, Perl, and Tcl as a tool for creating better scientific software (see <http://www.python.org>; <http://www.perl.org> and <http://www.tcl.tk>).

PY_Refdif_S is based on the Python scripting language. Python, as stated, is an interpreted, interactive, object-oriented programming language. The idea behind using Python was not only to solve the single computational domain limitation of Refdif_S but also to assess the suitability of Python for coastal processes research. The choice of the Python language was based on the following factors.

- (a) The fact that the language uses natural syntax – most Fortran/C programmers can understand the code structure on reading it.
- (b) It includes object-oriented programming, dynamic typing, regular expressions, etc.
- (c) There is strong community support of numerical libraries (Numeric, Numpy, Numarray, SciPy).
- (d) Interface software to combine Python with Fortran/C/C++ code exists (F2Py and Swig).
- (e) Numerous high-quality visualisation interfaces (VTK, Matplotlib, NCAR graphics, MayaVi); netCDF and HDF5 interfaces exist (PyTables, PyNGL, ScientificPython).
- (f) There is an extensive number of graphical user interfaces (wxPython, TKinter, Qt, etc.).
- (g) Cross-platform, code programmed in Windows, runs on Linux and macOS.
- (h) It is open-source.

At first, Python was used to prepare the data files, execute and create the results files of the model Refdif_S. Python was also used to enable Refdif_S to be applied to computational domains discretised by several finite-difference grids. The resulting tool was named PY_Refdif_S, which enabled the simulation of the propagation and shoaling of linear irregular waves in regions discretised by one or more finite-difference grids.

This software was then used to compute the inshore wave characteristics along the Torres-Mostardas beach, in Rio Grande do Sul, Brazil. The application of that tool to a real case scenario highlighted the requirements of this large model in terms of CPU time and memory storage. In fact, for only one incident irregular wave condition (spectrum) to be considered the regular wave Refdif model has to be executed for each of the spectral components of the incident spectrum. Usually, the spectrum is divided into 10×20 spectral components which correspond to 200 calculations. This is associated with a long CPU time and memory storage on the PC computer used on LNEC. Moreover, other tasks on the PC computer cannot be performed while the computations are running.

The solution for this problem was to run PY_Refdif_S on a dedicated machine. Hence, an extension, also written in Python, was also implemented to automate this task.

The routines developed on Python are mentioned below.

2.2.2. *Simulation of large areas.* When applying the regular wave model Refdif, it is common to discretise the domain with

several grids with different characteristics and execute the model in sequence for each grid taking into account the transfer of wave information between grids. This methodology is especially applied when large study areas are involved. All grids have the same properties of the grids used in a regular Refdif model; that is, they are rectangular grids with all grid elements identical and the size of the grid elements depends on the bathymetry present in the computational domain and on the wave period. The criteria for usage of additional grids are identical. Typically, as the grids approach the shore the smaller the grid spacing will be, since lesser depths are present.

As mentioned, in the irregular wave model Refdif_S, this was not possible and so several Python routines were developed in order to run Refdif for each spectral component, in each grid that discretises the computational domain.

This methodology consists of the following steps.

- (1) Compute the spectral components (i, j) of the incident wave at the first grid, being i the frequency component and j the directional component. For this purpose, Specgen routine is used.
- (2) For the first grid (with dimensions $m_r \times n_r$), execute Refdif for each of the spectral components and
 - (a) for each spectral component (i, j), store in a vector, $(\mathit{owave}_n)_{i,j}$, the values for complex wave amplitude, $(A_{m_r,n})_{i,j}$, corresponding to each point (m, n) of the last row of the grid, where $m = m_r$ and n varies from 1 to n_r .
 - (b) Combine the results of all the spectral components.
 - (i) For the first spectral component
 - compute the square of the modulus of the complex wave amplitude in each point of the grid (m, n), that is $|(A_{m,n})_{1,1}|^2$
 - store the previously computed value, $|(A_{m,n})_{1,1}|^2$, in a matrix, $S_{m,n}$.
 - (ii) For the remaining spectral components
 - compute the square of the modulus of the complex wave amplitude at each point of the grid (m, n), $|(A_{m,n})_{i,j}|^2$
 - add the computed values of $|(A_{m,n})_{i,j}|^2$ to the matrix $SA_{m,n}$. Hence, in the end, the result will be

$$1 \quad SA_{m,n} = \sum_{i=1}^{N_f} \sum_{j=1}^{N_\theta} |(A_{m,n})_{i,j}|^2$$

- (c) After the superposition of the results for all the spectral components (N_f frequency components and N_θ directional components), compute the significant wave height for the first grid. This task is performed by the module Squaredroot. It computes the significant wave height, H_{m0} , in the following way

$$2 \quad H_{m0,m,n} \sqrt{8 \times \mathit{sumwave}_{m,n}} = \sqrt{8 \times \sum_{i=1}^{N_f} \sum_{j=1}^{N_\theta} |(A_{m,n})_{i,j}|^2}$$

- (3) Refdif is executed for the second grid.
 - (a) For each spectral component, use the results stored in the last row of the first grid, $(\mathit{owave}_n)_{i,j}$, as input values for the first row of the second grid.

- (b) For each spectral component, store the last row of results for the complex wave amplitude.
- (c) Superimpose the results of all the spectral components, using Equation 1.
- (d) After the superposition of the results for all the spectral components (N_f frequency components and N_θ directional components), compute the significant wave height for the second grid, using Equation 2.

For the remaining grids, the procedure (3) is repeated. An exception is made to the last grid where there is no need to store the results for the last row of complex wave amplitude. A diagram is presented in Figure 2.

2.2.3. *Remote execution.* As stated above, due to the long execution times of PY_Refdif_S a method to automate its remote execution on a dedicated server had to be implemented. Again, Python was used to perform this task. As a first approach, the solution adopted consisted in simply opening a file transfer protocol (FTP) connection for sending the program and data files, opening an interactive secure shell (SSH) connection and executing PY_Refdif_S remotely. When execution terminates, the result files are retrieved through an FTP connection, as can be seen in the activity diagram (Figure 3).

3. APPLICATION OF PY_REFDIF_S TO TORRES-MOSTARDAS

The PY_Refdif_S software tool was applied to study wave propagation along the Rio Grande do Sul coast, in Brazil, in the region between Torres and Mostardas (Figure 4). The objective of the study was to evaluate the irregular wave propagation behaviour from offshore to the nearshore and to transfer the offshore sea states of Fontoura (2004) to the coast. Notice this is a very large area which implies a large computational domain for the PY_Refdif_S software tool and consequently the use of several finite-difference grids. It therefore constitutes an excellent case to test the methodology here described.

The methodology used consisted of the following steps.

- (a) Definition of the offshore incident wave conditions of the model based on the offshore sea states of Fontoura (2004).
- (b) Wave propagation calculations with PY_Refdif_S for the different irregular incident wave conditions.
- (c) Use of the PY_Refdif_S software tool's results (significant wave heights) to characterise the wave field from offshore to inshore and to transfer the offshore sea states to the front of Torres-Mostardas beach (in fact, to point 7, which is a midpoint of the region between Torres and Mostardas, see Figure 9 later), enabling the local sea states.

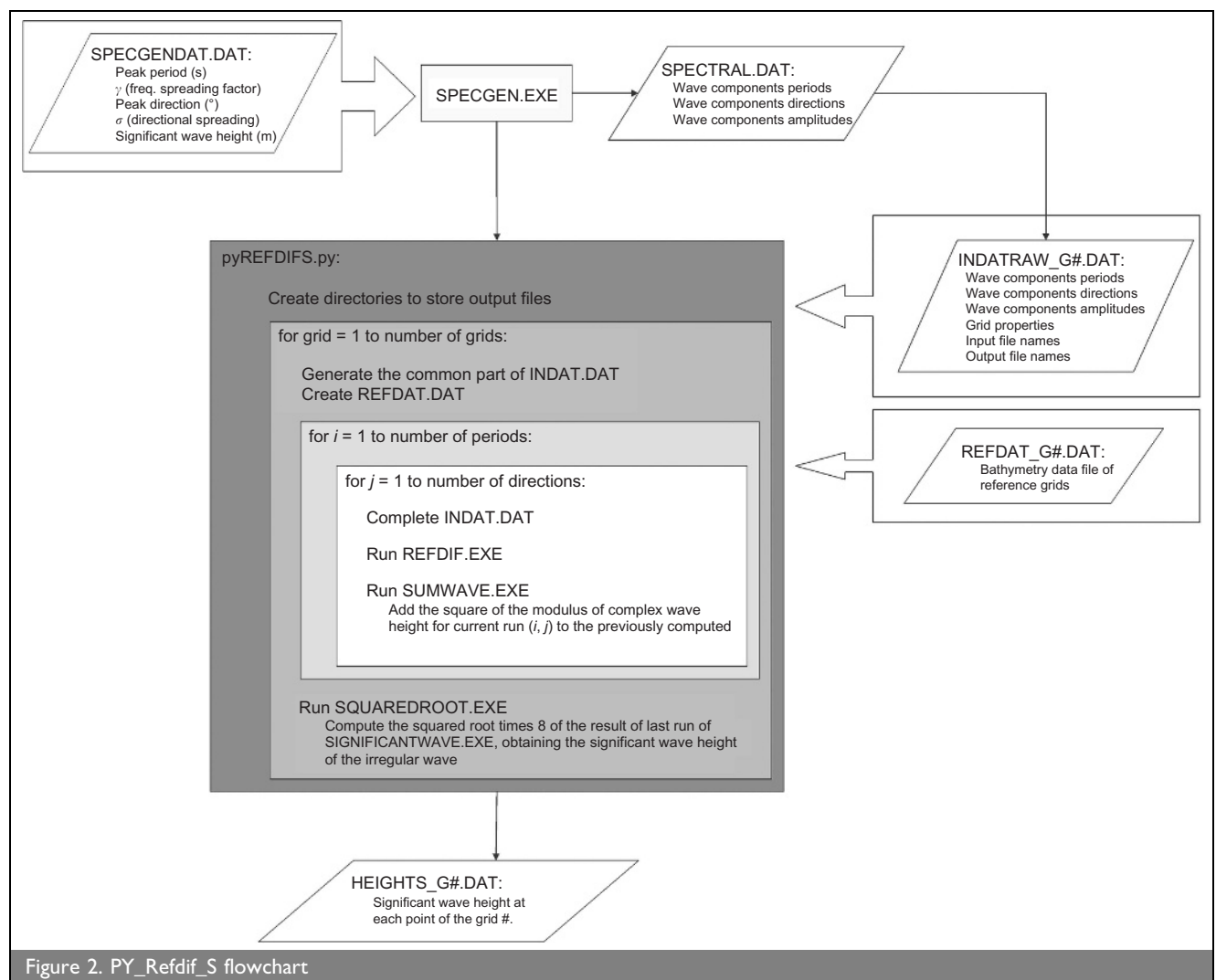
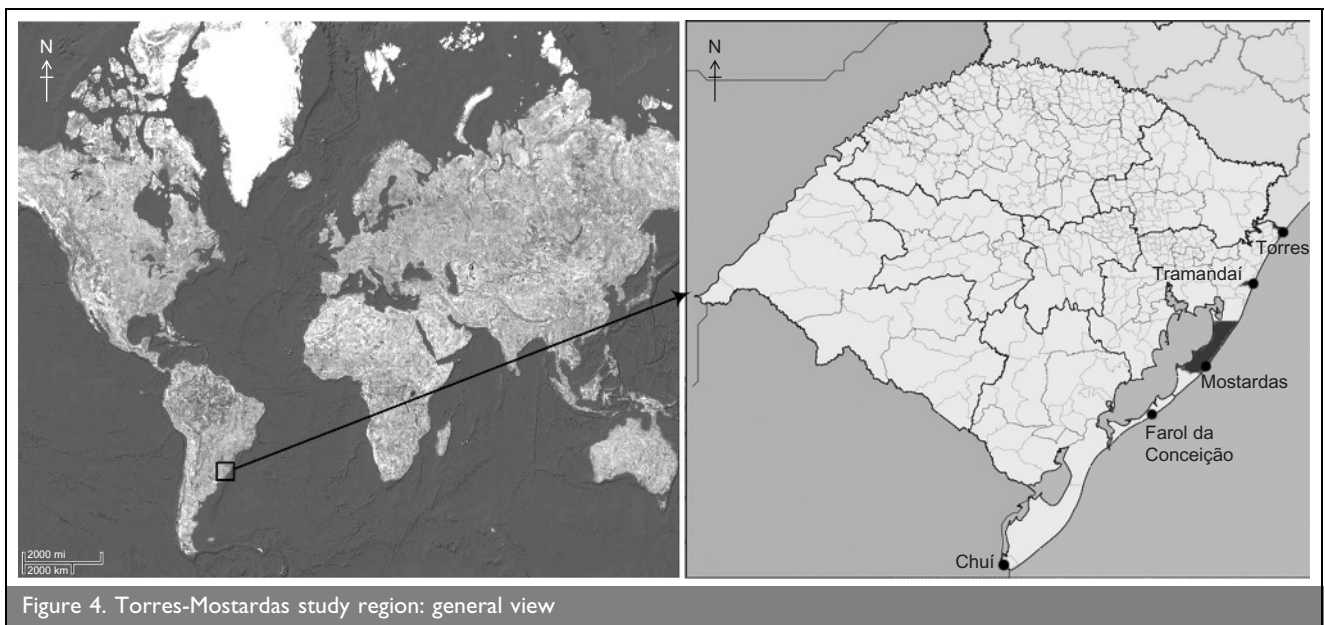
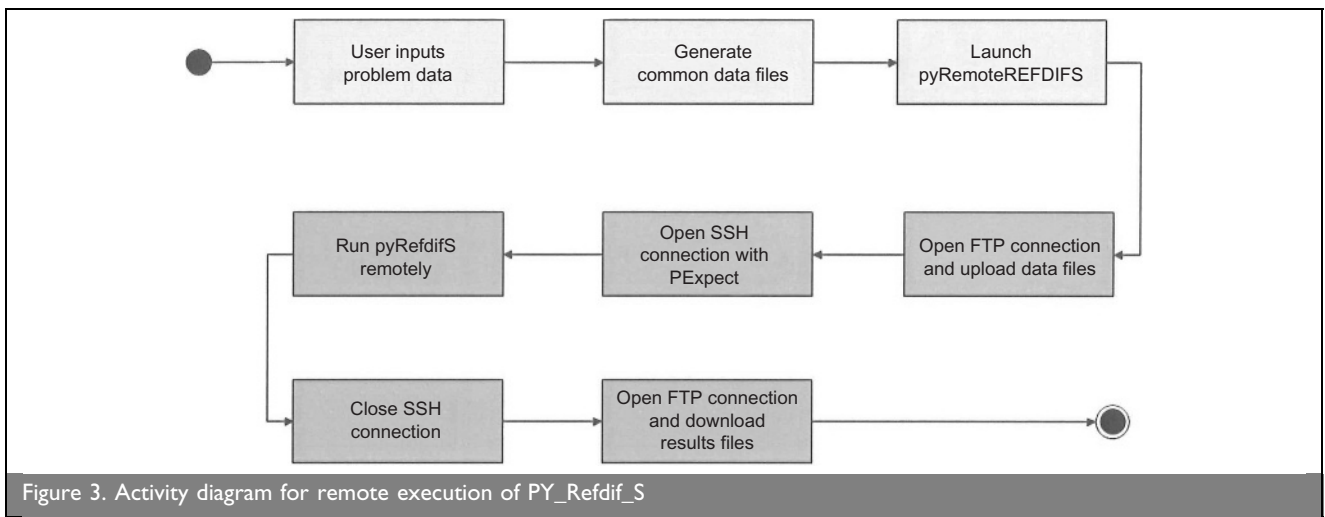


Figure 2. PY_Refdif_S flowchart



3.1. Study area

The Torres-Mostardas region is a very large 245 km long area. The continental shelf in this region is narrow, with a width of approximately 120 km (Figures 4 and 5) and the water depth contours are approximately parallel to the coast. In the same way, the wave refraction regime is very homogeneous, except for the region where a variation in the continental shelf width occurs. The coast from Torres to Tramandai is slightly concave with a Holocene barrier formed by a beach/foredune ridge strand plain ranging from 2 to 5 km wide. The westernmost ridge is highest and was interpreted as a transgressive barrier. From Tramandai to Mostardas the coastline is slightly convex-seaward; the barrier ranges from 2 to 6 km in width and is completely covered by transgressive dunes and in many places the dunes extend onto the Pleistocene barrier. There is no evidence of beach/foredune ridge strand plain.

3.2. Offshore sea states

Fontoura (2004) presents offshore sea states (wave height, wave period and wave direction) based on the daily results obtained by the National Institute for Space Research (INPE, Brazil) using the third-generation wave model Wavewatch III (Tolman, 1999).

This model uses the wind fields previewed by the Mesh Global Atmospheric Model (MCGA) for the coordinates of $32^{\circ} 0' 0''$ S and $48^{\circ} 45' 0''$ W. Only the results of the MCGA concerning the significant wave height (H_s), mean wave period (T_z) and mean wave direction (Θ) were considered by that author.

The above results, taken every hour, refer to the period from 26 September to 25 December 2001 (almost 3 months). Figure 6 shows the chronological time series of H_s , T_z and Θ for the study period of 3 months. This constitutes the offshore sea states considered in this study.

Data on Figure 6 show that T_z varied between 4 and 12 s, H_s varied between 0 and 6 m and Θ varied between 0 and 360° . Notice also that from 26 September to 18 November, there were no significant gaps on the measurements, which did not happen in the rest of the period of observation.

Based on the above data, a statistical analysis was made, namely the root mean squares of the H_s , T_z and Θ values for each day were evaluated. These values, as well as corresponding histograms, are presented in Figures 7 and 8.

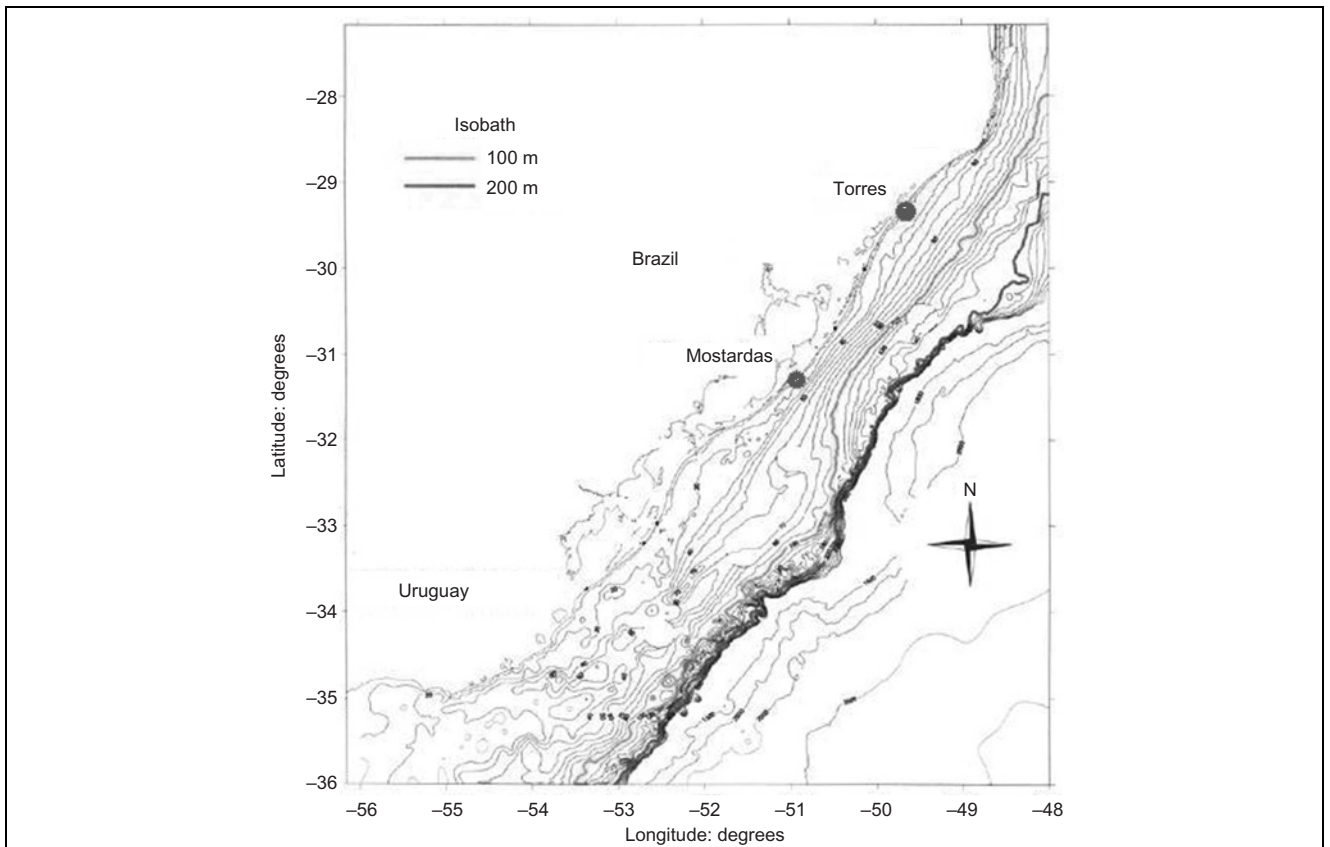


Figure 5. Torres-Mostardas study region: bathymetry

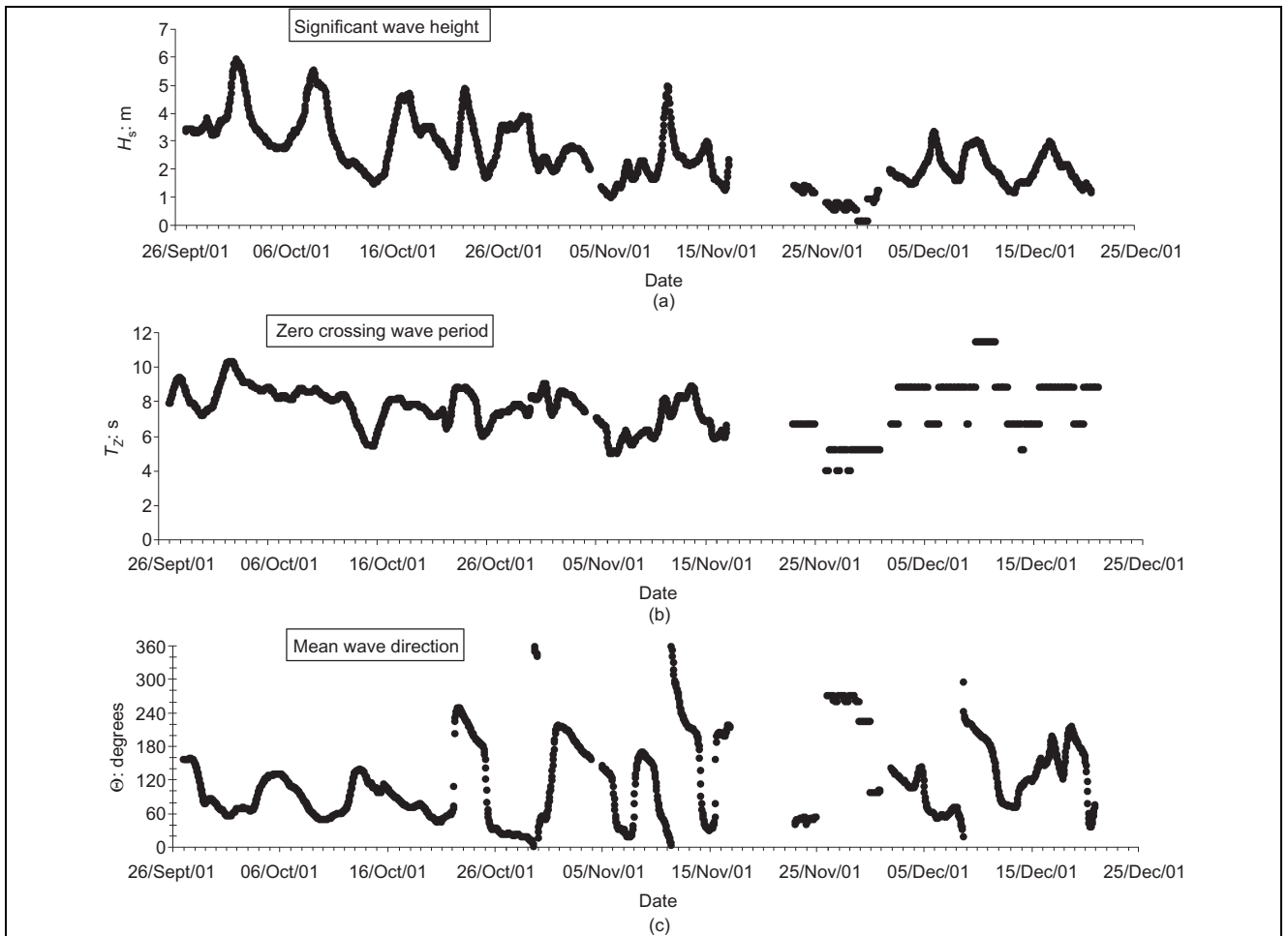


Figure 6. Time series of the offshore H_s , T_z and Θ from 26 September 2001 to 25 December 2001

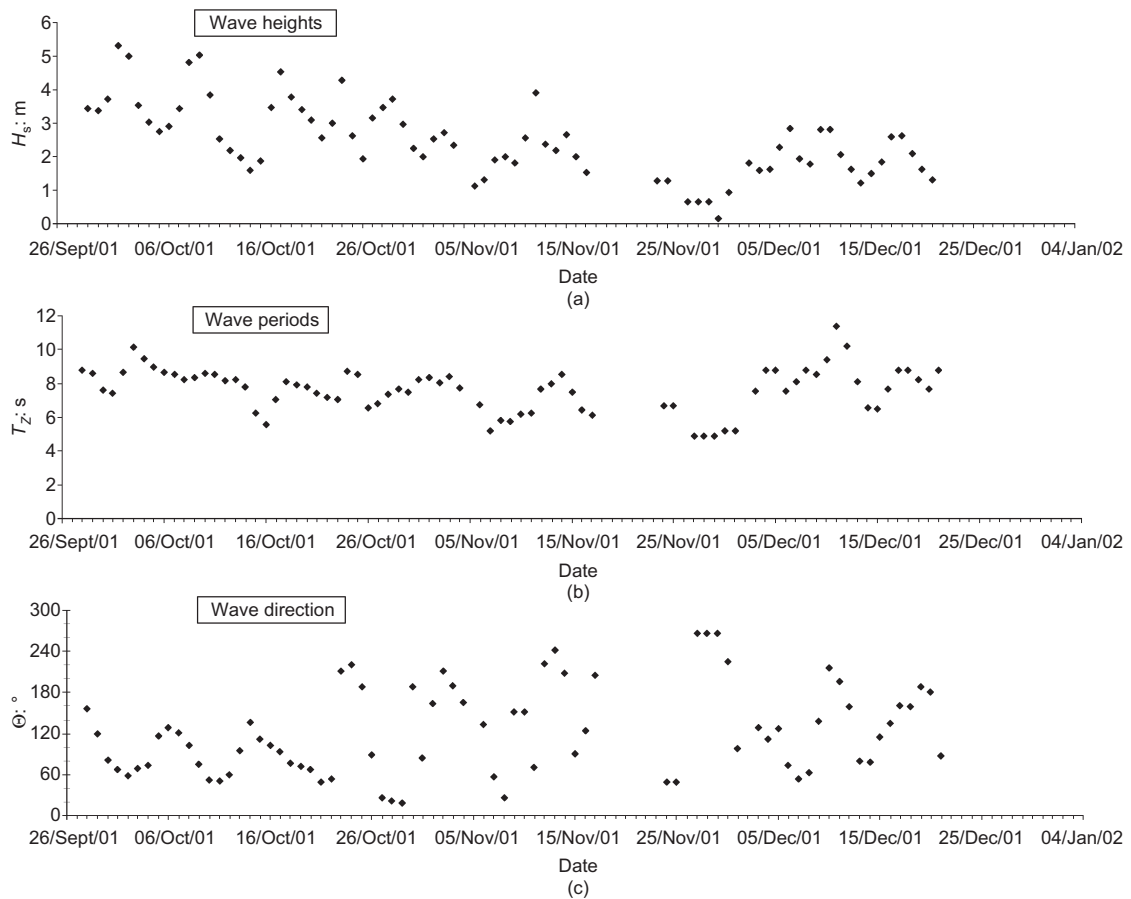


Figure 7. Daily average of H_S , T_Z and Θ in deep water, from 26 September 2001 to 25 December 2001

As shown in Figure 7, the root mean square of the H_S varied between 0.14 and 5.32 m, the root mean square values of T_Z were between 4 and 12 s and the root mean square values of Θ were between 19° and 265°. The histograms in Figure 8 show

that: (a) the most frequent root mean square of the significant wave heights were associated with the range between 1.5 and 4.0 m (~76%); (b) the frequent wave periods (~83%) were in the range between 6.0 and 10 s; (c) the most frequent wave

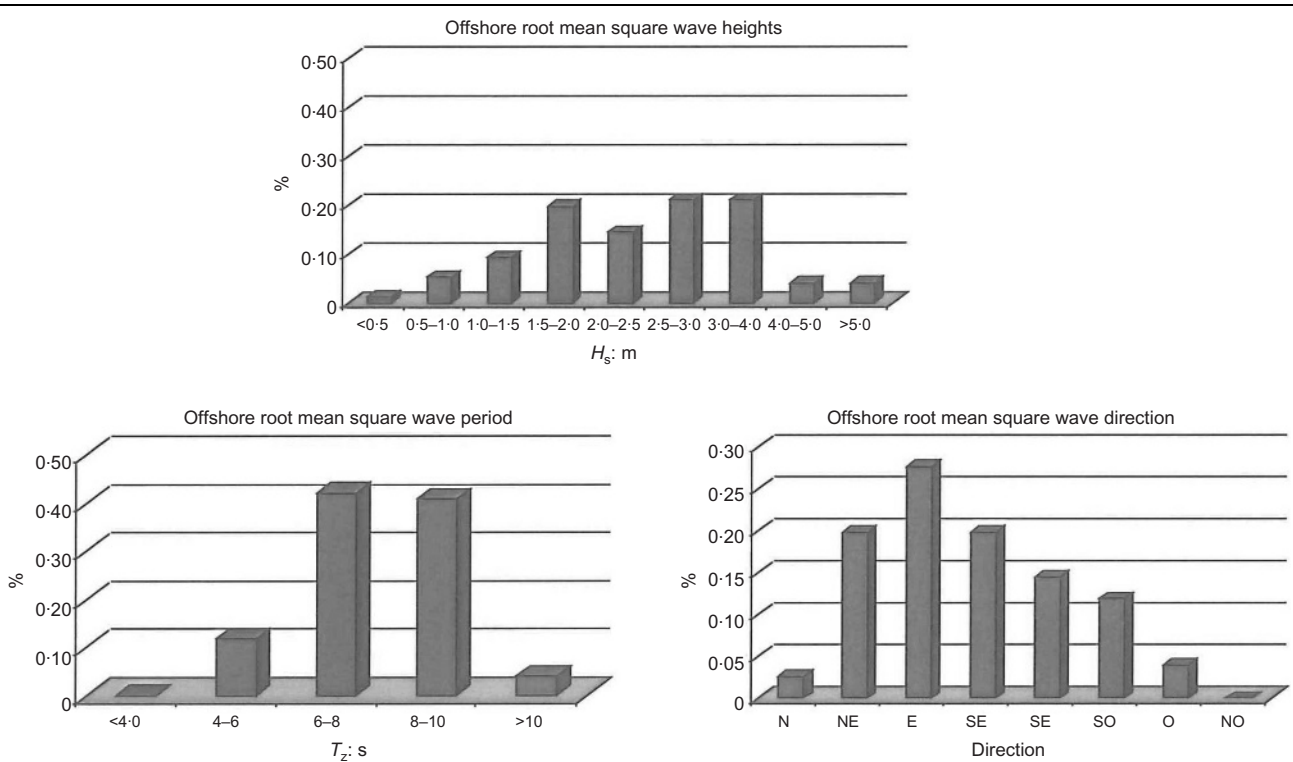


Figure 8. Histograms of the daily average of H_S , T_Z and direction in deep waters, from 26 September 2001 to 25 December 2001

directional distribution function of Borgman (1985) were considered. The frequency spectrum and the directional distribution function were the ones available at the Refdif_S model and as no studies or data were available for this study area, these were the formulations adopted in the present study. The characteristics of the frequency and direction spectrum were based on the data presented in Figures 6 to 8.

- (a) The mean wave directions considered for each directional distribution function were south (S; 180°) to north-east (NE; 45°), spaced by 45° (four mean wave directions, S, SE, E and NE). This range of wave conditions corresponds to those which can be propagated from offshore to inshore and arrive at the study area of Torres Mostardas.
- (b) The peak periods (which correspond approximately to $T_p = 1.27T_z$ for the TMA spectrum) considered for each frequency spectrum were $T_p = 5, 6, 7, 8, 9, 10, 11$ and 12 s. This range corresponds to the most frequent periods, in general. The entire range of wave periods was not considered in order to avoid a significant increase in computer calculations.

The frequency and direction spectra were divided into 10 different frequency components and 20 different directions. The offshore directional spectrum parameters considered were $\gamma = 20$ and $\sigma = 10$ as recommended by Zózimo *et al.* (2001) for narrow spectra. As noted by Zózimo *et al.* (2001) these coefficients have little effect on the accuracy of the results but wider spectra significantly increase the computation time. This is the reason why a narrow spectrum was chosen.

Considering that the H_s does not influence the ratio between the offshore significant wave height and the computed significant wave height nearshore with PY_Refdif_S, as shown in previous studies (Fortes *et al.*, 2007), in the present study it was considered sufficient to consider only one wave height, in order

to avoid a significant increase in computer calculations. Hence, although any wave height could be used, nevertheless $H_s = 1.75$ m was chosen since it corresponds to one of the most frequent significant wave heights.

The tide level considered was 0.22 m which corresponds to the average tide level.

The hydrographic survey and the grids used for each of the wave conditions selected are presented in Figure 9.

Due to the large study area, for each incident wave direction (NE and SE), three different finite-differences grids were defined. On the definition of the dimensions and resolution of those grids, the following aspects were taken into account.

- (a) The grid spacing is defined in order to guarantee a minimum of five grid points per wave length, as specified in Refdif's user manual (Dalrymple and Kirby, 1991). However, one should also take into account the computer resources.
- (b) The orientation of the grid should guarantee that the wave direction inside the grid does not exceed $\pm 60^\circ$ of the principal wave direction. In this work a 45° orientation was adopted.

The main characteristics of the grids used are presented in Table 1.

Note that x is the main propagation direction of waves (NE x , NE y , SE x or SE y , see Figure 9) and y is the transversal wave direction (NE y , NE x , SE y or SE x , see Figure 9). The points N1, N2, N3, S1, S2 and S3 are the grid points shown at Table 1. L_x and L_y are the lengths of the grids on the direction x and y , respectively. Δx and Δy are the grid spacing on the x and y directions, respectively. N_x and N_y are the number of elements of the grids on the x and y directions, respectively.

	Direction	NE	E	SE	S
Grid 1	S1 _x	650 522	624 156	638 000	610 000
	S1 _y	6 716 264	6 658 112	6 643 000	6 573 000
	L _x : m	41 856	30 720	25 008	29 760
	L _y : m	89 856	45 072	69 984	54 240
	Θ _x : m	48	24	48	48
	Θ _y : m	48	24	48	48
	N _x	873	1281	522	621
	N _y	1873	1879	1459	1131
Grid 2	S2 _x	615 894	593 439	609 727	607 216
	S2 _y	6 683 779	6 655 616	6 650 094	6 602 760
	L _x : m	33 024	27 840	14 976	24 000
	L _y : m	62 976	40 080	40 008	43 200
	Θ _x : m	24	24	24	24
	Θ _y : m	24	24	24	24
	N _x	1377	1161	625	1001
	N _y	2625	1671	1668	1801
Grid 3	S3 _x	585 983		595 608	603 736
	S3 _y	6 667 813		6 657 153	6 626 760
	L _x : m	24 960		15 000	30 720
	L _y : m	34 992		30 000	36 240
	Θ _x : m	24		24	24
	Θ _y : m	24		24	24
	N _x	1041		626	1281
	N _y	1459		1251	1511

Table 1. Finite-difference grids characteristics

3.4. Results

For the above model conditions, a total of 32 calculations with PY_Refdif_S were performed, which correspond to 32 different offshore irregular wave conditions (8 periods \times 4 directions \times 1 wave height). For each irregular wave calculation, 200 spectral component calculations (10 frequencies \times 20 directions) were performed. So a total of $200 \times 32 = 6400$ calculations were performed.

The CPU time of each irregular wave calculation performed by PY_Refdif_S, for 200 spectral components ($N = N_f \times N_\theta$), was 50 h 20 min, which corresponds on average to a mean calculation time of each spectral component (regular wave) of 15 min. The total time of the 6400 calculations was approximately 59 days. The calculations were performed in a dedicated server: an AMD Athlon™ Dual Core Opteron 1.7 GHz, 2.00 GB of RAM, using serial code. The use of a supercomputer with more cores and parallel executions would reduce the calculation time even more.

Previously, the computations were performed on a personal computer AMD Athlon™ XP3000+ 2.17 GHz, 1.00 GB of RAM, taking 83 h 20 min for the computation of 200 spectral components, an average of 25 min for each spectral component.

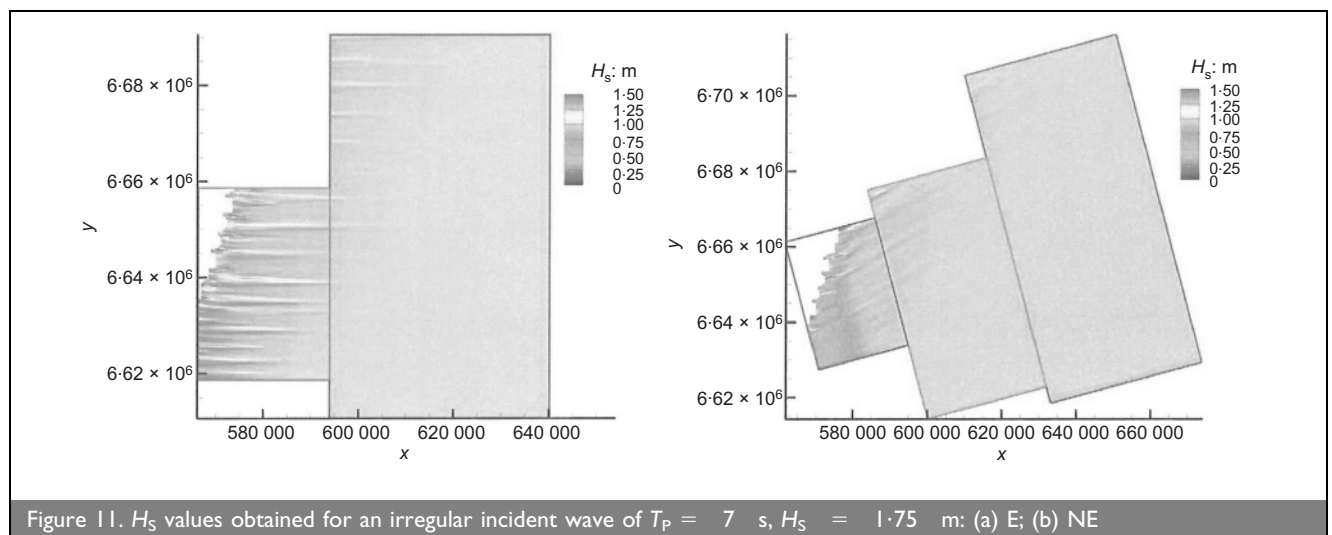
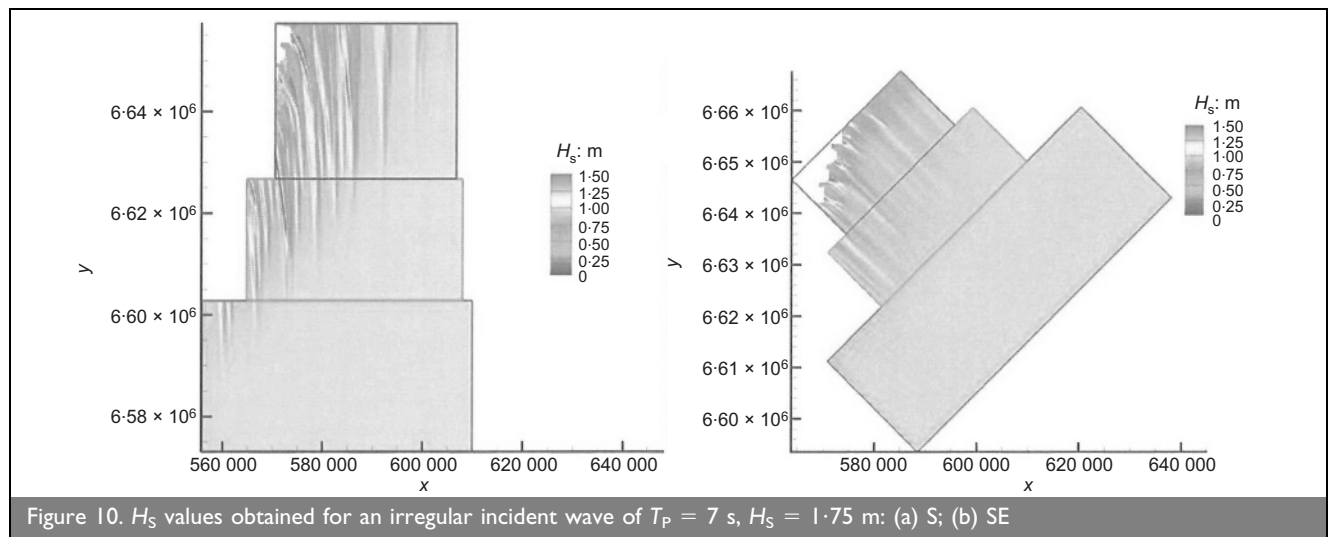
The results of PY_Refdif_S consist of the values of the

significant wave heights along the whole domain and at several points along the bathymetric contours of -7 and -10 m (Figure 9).

3.4.1. General view. Figures 10 and 11 present the significant wave height values from offshore to inshore, obtained with the PY_Refdif_S software tool, for the offshore wave directions of NE, E, SE and S, $H_0 = 1.75$ m and the peak wave period $T_p = 7$ s.

From Figures 10 and 11 it can be seen that the incident waves do not suffer the effects of the bottom, until a depth of approximately 45 to 50 m (second grid or eventually on the third grid). For smaller bottom depths, the waves progressively rotate towards a direction perpendicular to bathymetric contours, therefore there are significant modifications on the wave heights. Along the coast, there are some zones of energy convergence, depending on the incident wave, and in addition to that, wave breaking occurs.

One notices also that the beach is more exposed to wave action when the incident wave direction ranges between NE and E. In general there are more energy convergence areas for the E incident wave direction than for NE. There are no major differences on the magnitude of the significant wave heights when the waves range between E and SE. Between SE and S, there is a slight decrease in the significant wave height, but there



are still some energy convergence areas. In general, there are less energy convergence zones for the offshore directions of NE than for other directions. The situation of the convergence zone at the coast varies with the offshore wave direction, as expected.

Figure 12 presents the wave height indices obtained at all the points P1 to P7 calculated by the PY_Refdif_S software tool, in function of the wave direction and the wave period, for an incident wave height of $H = 1.75$ m.

Points 1 to 15 are on the 5 m depth contour and points 16 to 29 are on the 10 m depth contour. In general, there are no significant differences between the offshore and inshore wave heights, for incident wave directions of 45 to 135°; that is, the wave height indexes are around 1.0. This is due to the orientation of the bathymetry.

In relation to the incident wave direction of 180°, the differences are more significant. In general, the wave heights decrease as the wave propagates shoreward. Notice that for this direction the wave has to refract a lot and so there is a decrease of the wave heights.

3.4.2. *Sea states at point 7.* Using the results of PY_Refdif_S, especially those obtained at point 7 (Figure 9), the offshore data (Figure 6) is transferred to inshore, defining local sea states at that point. This point was chosen due to the fact that it is located in the midpoint of the region Torres-Mostardas. Basically, the following steps were adopted.

- (a) Use of offshore sea states based on data of Fontoura (2004).
- (b) Use of PY_Refdif_S, to obtain a transfer matrix from the offshore wave data (H_S , T_Z , Θ) to point P7.
 - (i) Run PY_Refdif_S for 20 ($1 \times 5 \times 4$) different wave conditions: $H_S = 1.75$ m; $T_Z = 5, 6, 7, 8$ and 10 s; $\Theta = 45, 90, 135$ and 180°.
- (c) Definition of the local sea states at point 7.
 - (i) Extrapolate PY_Refdif_S computations to obtain a regular matrix of $1 \times 8 \times 9$ (72) elements: $H_S = 1$ m;

$T_Z = 4, 5, 6, 7, 8, 9, 10$ and 11 s; $\Theta = 22.5, 45, 67.5, 90, 112.5, 135, 157.5$ and 180°.

- (ii) Transfer all offshore records from 26 September 2001 to point P7.
- (iii) Transfer daily offshore root mean square records to point P7.

This methodology can be used to establish local sea states at any other point.

Figure 13 presents the extrapolated transfer matrix for point 7, for an incident wave height of $H = 1.75$ m. It is assumed that there is no influence between the offshore and the inshore wave heights; therefore all offshore wave height data are divided by 1.75 and after the transference to point P7 they are multiplied by its original value.

In general, there are no significant differences between the offshore wave heights and the inshore, for incident wave directions between 40 and 140°. There is a slight decrease of the wave heights for the short periods and a small increase for the higher periods, due essentially to shoaling and refraction effects. For wave directions between 150 and 180° there a significant decrease of the incident wave heights, for all periods, since for those directions the angle between the orthogonals and the bathymetry is very small (refraction effects). This effect can be explained theoretically for straight and parallel isobaths with energy conservation laws (linear shoaling) and Snell's law (refraction) (Dean and Dalrymple, 1984).

Figure 14 presents the transferred time series of H_S from 1 October 2001 to 31 October 2002 at point P7. For comparison purposes, the offshore data are also presented.

Figure 14 shows that there are not so much modifications in the significant wave heights from offshore to inshore but, in general, there is a reduction of H_S . There are some gaps in the transferred values since it was not possible to transfer all the

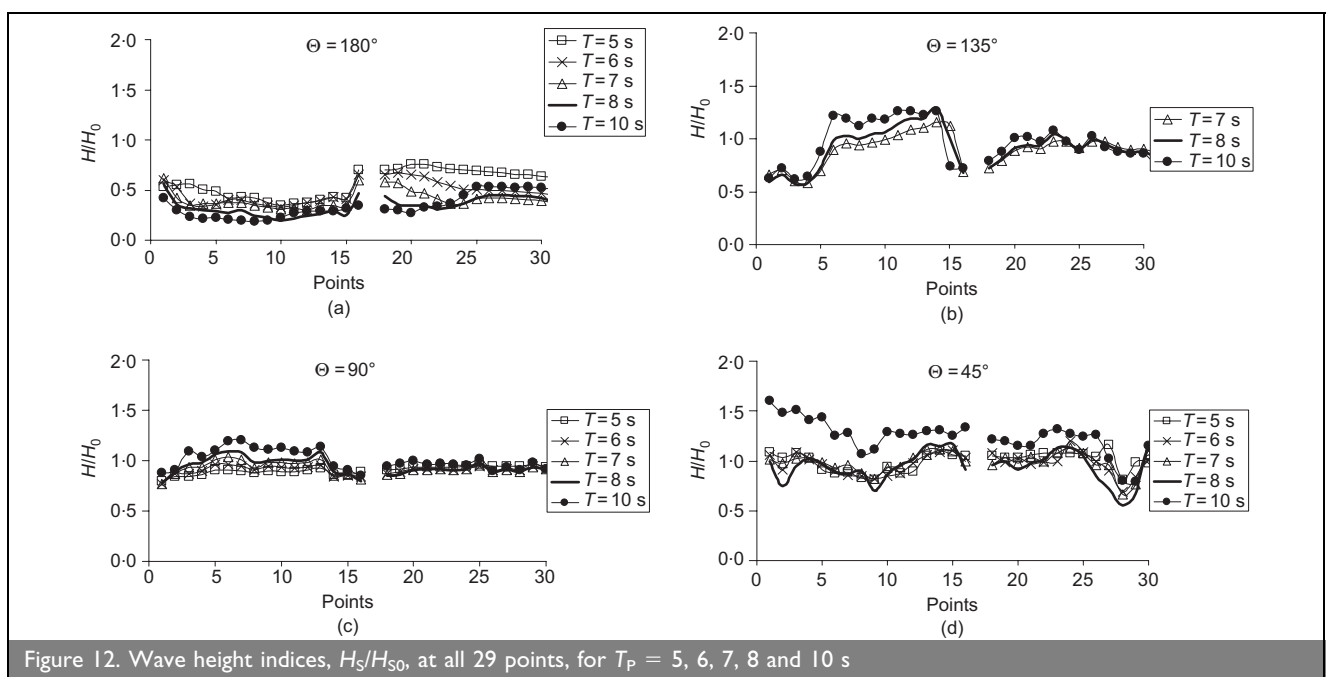
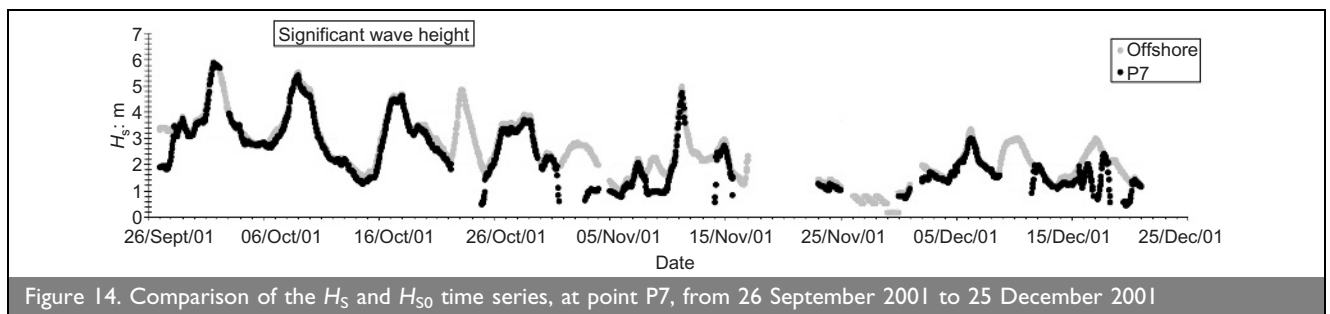
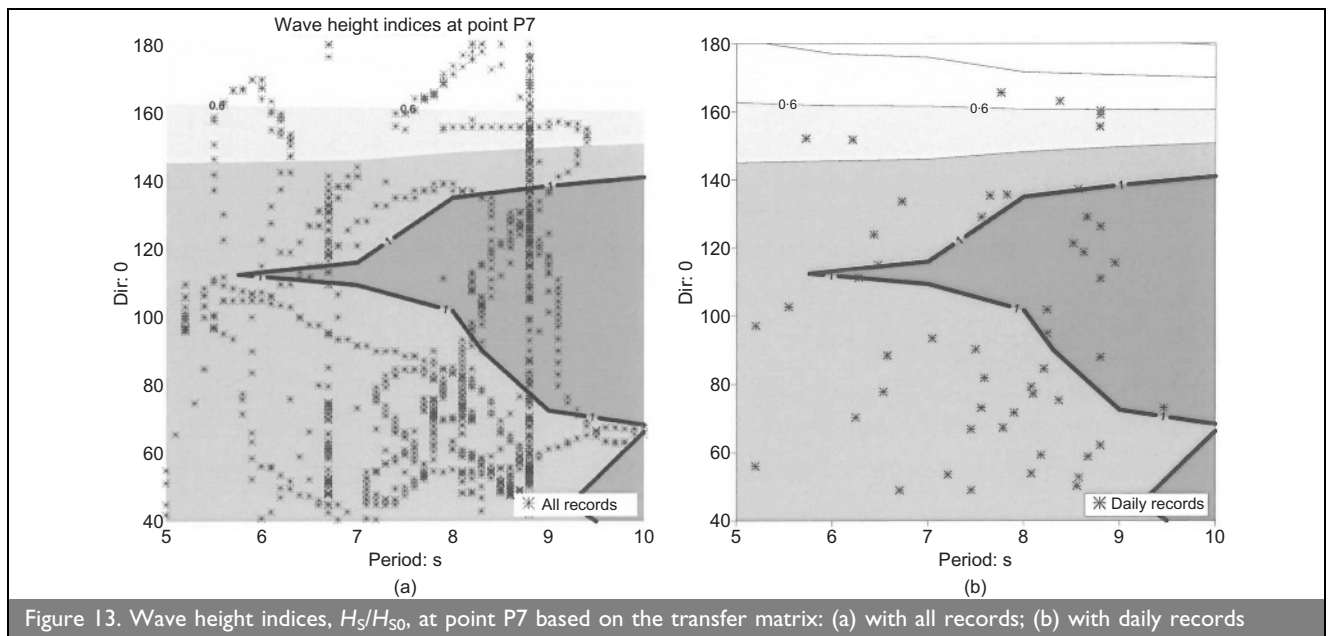


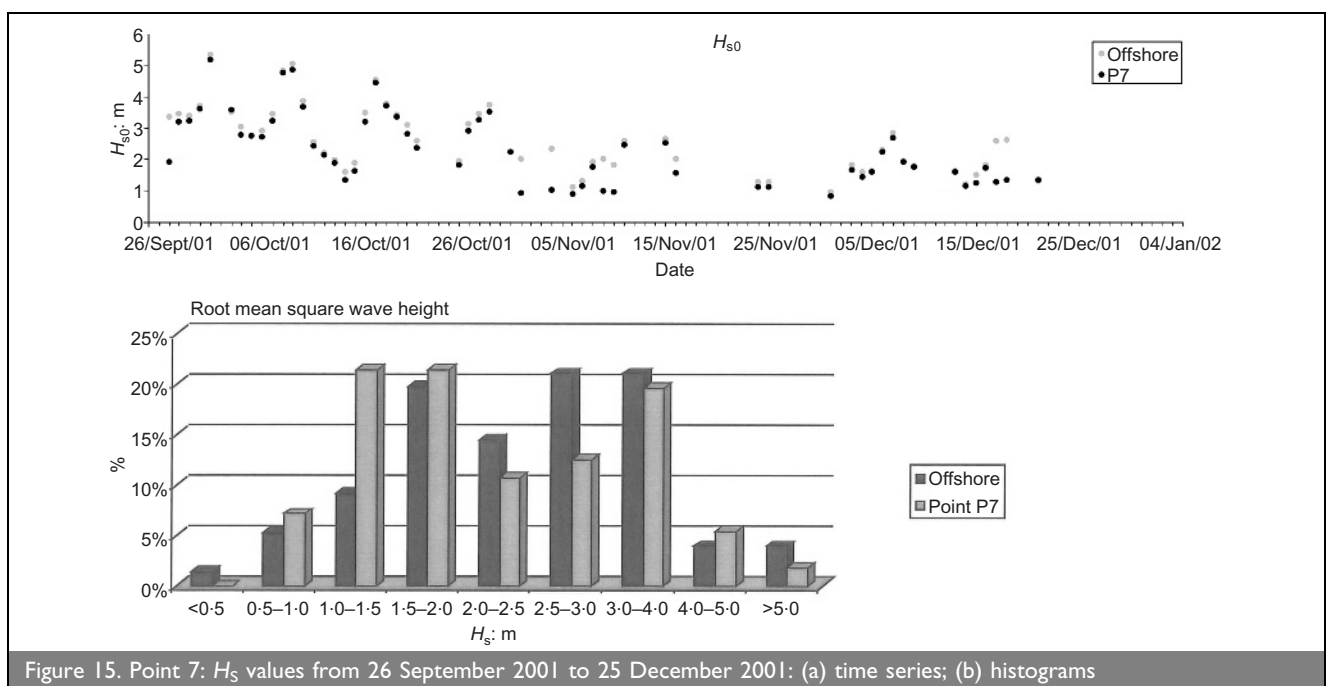
Figure 12. Wave height indices, H_S/H_{S0} , at all 29 points, for $T_P = 5, 6, 7, 8$ and 10 s



values of the offshore data, since some of the values are outside the bounds of the transfer matrix.

As for the offshore data, a similar analysis was also made for the significant wave height results at point P7. The root mean

squares of the significant wave heights were calculated for each day. Histograms for these values are shown in Figure 15(b). As shown in Figure 15(a), the root mean square of the significant wave heights varies between 0.83 and 5.16 m. In the histogram (Figure 15(b)), the most frequent root mean squares of the



significant wave heights at point P7 are associated with the range 1.0 to 2.0 m (~43%) whereas in the offshore data they were associated with the range 2.5 to 4.0 m (~42%).

4. CONCLUSIONS

In this paper, a methodology to extend the applicability of the Refdif_S model to propagate irregular waves over very large regions was presented. This was achieved by using the Python programming language, through the development of several Python routines that perform the automatic preparation of data files of the model, its execution on a Unix workstation instead of a personal computer and the transfer of results and data between the Windows and Unix environments. Moreover, the application of the model in large areas is also achieved by using several finite-difference grids to discretise the whole area of interest. The resulting software tool is named PY_Refdif_S.

This example demonstrates the flexibility of this programming language in the solution of problems of this kind that demand the interaction and communication between different software modules.

The PY_Refdif_S tool was applied to study the propagation of irregular waves from offshore to the region of Torres Mostardas at Rio Grande do Sul, Brasil. It was also used to transfer the offshore data presented by Fontoura (2004) to the bathymetric of -5 m in front of Torres-Mostardas beach. Notice that Torres-Mostardas is a very large area where only the PY_Refdif_S software tool made it possible to propagate irregular waves in such a large area.

The model was applied with the mean yearly tide level and for a range of irregular waves which were established based on the data presented by Fontoura (2004). Calculations were performed from offshore to nearshore in the region of Torres-Mostardas for peak periods in the range 5 to 10 s and mean wave directions between S and NE, using a significant wave height of 1.75 m.

The application of the model showed that the incident wave does not suffer the effects of the bottom, until a depth of approximately 45–50 m. For smaller bottom depths, the waves progressively rotate towards a direction perpendicular to bathymetric contours, and so there are significant modifications in the wave heights. Along the coast, there are some zones of energy convergence, depending on the incident wave, in addition to that, wave breaking occurs. In general, the beach is more exposed to the wave action when the incident wave direction ranges from NE to E and from S to SE.

Beside the great advantages of the PY_Refdif_S tool here presented (application to large areas, irregular wave propagation considering refraction, diffraction and wave breaking, an important CPU time and memory storage saving), there are still some limitations that restrict the general application of the model. In general, they are related to the limitations of the theoretical aspects on which the Refdif model is based: it is not possible to propagate incident waves which will lead to inshore wave directions that are outside the interval $\pm 60^\circ$ of the principal incident wave direction; for certain short periods, the grid associated is so fine that it invalidates the computation of those periods; it is not possible to model nonlinear effects, such as energy transfer between spectral components, the generation

of harmonics, since the Refdif_S model is based on the linear superposition of the wave solutions; it is yet not possible to calculate the mean wave directions after the propagation with the PY_Refdif_S tool.

These aspects limit the incident waves that can be propagated from offshore to inshore. The improvement of these aspects constitutes one of the objectives of the future work. Moreover, there is the intent to use a Matplotlib Python module to generate the output graphics. The idea behind this is not only the automation of the generation of graphics but also the possibility to have a stand-alone framework that does not depend on proprietary software for data visualisation.

ACKNOWLEDGEMENTS

Financial support from the Portuguese Research Council, through POCTI projects POCTI/CTA/48065/2002 and POCTI/EME/47576/2002 is gratefully acknowledged. This work was the result of a collaboration between LNEC and FURG.

The authors would like to thank João Alfredo Santos and Dr Mendes de Carvalho for reviewing the text.

REFERENCES

- Berkhoff JCW (1972) Computation of combined refraction–diffraction. *Proceedings of the 13th International Conference in Coastal Engineering, Vancouver*. ASCE, New York, NY, USA, vol. 2, pp. 471–490.
- Booij N, Ris RC and Holthuijsen LH (1999) A third-generation wave model for coastal regions, part I: model description and validation. *Journal of Geophysical Research* **104(4)**: 7649–7666.
- Borgman LE (1985) *Directional Spectrum Estimation for the Sxy Gauges*. Coastal Engineering Research Center, Waterways Experiment Station, Vicksburg, MS, Technical report, pp. 1–104.
- Bouws E, Gunther H, Rosenthal W and Vincent CL (1985) Similarity of the wind wave spectrum in finite depth water. *Journal of Geophysical Research* **90(C1)**: 975–986.
- Dalrymple RA and Kirby JT (1991) *REFDIF 1 Version 2.3 Documentation Manual. Combined Refraction/Diffraction Model*. University of Delaware, Newark, DE, USA, CACR Report No. 91–92.
- Dean RG and Dalrymple RA (1984) *Water Wave Mechanics for Engineers and Scientists*. Prentice-Hall, Englewood Cliffs, NJ.
- Fontoura JAS (2004) *Hidrodinâmica Costeira e Quantificação do Transporte Longitudinal de Sedimentos não Coesivos na Zona de Surfe das Praias Adjacentes aos Molhes da Barra do Rio Grande, RS, Brasil*. PhD thesis, Instituto de Pesquisas Hidráulicas, Universidade Federal do Rio Grande do Sul.
- Fortes CJEM, Pinheiro LV and Palha A (2007) SOPRO package: recent evolutions. *Proceedings of the 5th Portuguese Days of Ports and Coastal Engineering, Lisbon* (in Portuguese).
- Goda Y (1985) *Random Seas and Design of Maritime Structures*. University of Tokyo Press, Tokyo, Japan.
- Grassa JM (1992) *Modelos Parabólicos de Propagación de Oleaje*. Centro de Estudios y Experimentación de Obras Públicas CEDEX, Madrid, Spain.
- Ilic S and Chadwick AJ (1995) Evaluation and validation of the mild slope evolution equation model using field data. *Proceedings of the Coastal'95 Conference, Gdansk, Poland*. ASCE, New York, NY, USA, pp. 149–160.

- Kirby JT (1986) Rational approximations in the parabolic equation method for water waves. *Coastal Engineering* 10: 355–378.
- Kirby JT and Ozkan HT (1994) *REF/DIF S Version 1.1 Documentation and Users Manual*. University of Delaware, Newark, DE, USA, CACR Report No. 94-04.
- Kirby JT, Wei G and Chen Q (1998) *FUNWAVE 1.0 Fully Nonlinear Boussinesq Wave Model. Documentation and User's Manual*. University of Delaware, Newark, DE, USA, Rel.CACR 98 06.
- Lee HS and Williams AN (2002) Boundary element modelling of multidirectional random waves in a harbor with partially reflecting boundaries. *Ocean Engineering* 29(1): 39–58.
- Li B, Reeve DE and Fleming CA (1993) Numerical solution of the elliptic mid-slope equation for irregular wave propagation. *Coastal Engineering* 20(1–2): 85–100.
- Lynett P and Liu PLF (2004) A two-layer approach to water wave modeling. *Proceedings of the Royal Society of London A* 460(2049): 2637–2669.
- Panchang VG, Wei G, Pearce BR and Briggs MJ (1990) Numerical simulation of irregular wave propagation over shoal. *Journal of Waterways, Port, Coastal and Ocean Engineering, ASCE* 116(3): 324–340.
- Thornton EB and Guza RT (1983) Transformation of wave height distribution. *Journal of Geophysical Research* 88: 5925–5938.
- Tolman HL (1999) *User Manual and System Documentation of WAVEMATCH-III Version 1.18*. NOAA/NWS OMB. National Oceanic and Atmospheric Administration, Washington, DC, USA, Contribution No. 166, pp. 1–110.
- Vincent CL and Briggs MJ (1989) Refraction–diffraction of irregular waves over a mound. *Journal of Waterways, Port, Coastal and Ocean Engineering, ASCE* 115(2): 269–284.
- Walkley MA (1999) *Numerical Method for Extended Boussinesq Shallow-water Wave Equations*. PhD thesis, University of Leeds School of Computer Studies.
- Zózimo AC (2003) *Modelo de Elementos Finitos para a Propagação e Deformação de Ondas Irregulares em Zonas Costeiras*. Master's thesis, IST Lisbon, pp. 1–155 (in Portuguese).
- Zózimo AC, Fortes CJEM and Neves MG (2001) *Irregular Wave Propagation Model in Harbour Areas*. LNEC, Lisbon, Report 284/01 NPP-DH, pp. 1–56 (in Portuguese).

What do you think?

To discuss this paper, please email up to 500 words to the editor at journals@ice.org.uk. Your contribution will be forwarded to the author(s) for a reply and, if considered appropriate by the editorial panel, will be published as discussion in a future issue of the journal.

Proceedings journals rely entirely on contributions sent in by civil engineering professionals, academics and students. Papers should be 2000–5000 words long (briefing papers should be 1000–2000 words long), with adequate illustrations and references. You can submit your paper online via www.icevirtuallibrary.com/content/journals, where you will also find detailed author guidelines.